RESEARCH ARTICLE

Macromolecular Materials and Engineering
Open Access
www.mame-journal.de

Effect of Fluorine and Copper Ions on Liquid-Solid Triboelectric Nanogenerator

Mohamed Salman, Vladislav Sorokin, Zifan Li, Yuting Zhu, Wee Chen Gan, and Kean Aw*

Liquid-solid triboelectric nanogenerator (LS-TENG) harvests energy efficiently while eliminating wear issues associated with solid-solid TENG. However, the effect of ions or charges in the liquid on output performance needs further examination. In this work, the impact of fluorine and copper ions introduced through deionized water with sodium fluoride (DI-NaF) and deionized water with copper sulfate (DI-$CuSO_4$) solution on the output voltage, charge and current of a tubular LS-TENG with polytetrafluoroethylene (PTFE) and Nylon as solid materials is examined. The results indicate that fluorine and copper ions have opposite effects on PTFE and Nylon LS-TENG's output. The fluorine (F^-) ions enhance the triboelectric effect and charge transfer in Nylon LS-TENG, increasing output, while they hinder the charge transfer process in PTFE LS-TENG, consequently decreasing its output. Conversely, the copper (Cu^{2+}) ions have a positive effect on the output of PTFE LS-TENG and a detrimental effect on Nylon LS-TENG's output. Moreover, the results indicate that LS TENG's output performance depends on the charges of solid and liquid triboelectric materials. Thus, this study provides insights into material-ion interaction in LS-TENG and underscores the importance of triboelectric material selection for optimizing output performance.

1. Introduction

Increasing global energy demand, the rapid depletion of fossil fuels and their negative impact on the environment have shifted the focus to alternative, sustainable and renewable energy sources. As a result, much research has been carried out over the last decade on clean and sustainable energy harvesting from renewable energy sources such as wind, solar, geothermal, etc.[1] Devices that convert ambient mechanical energy, such as vibrational and ocean wave energy, into electricity have been gaining increasing attention. The triboelectric nanogenerator (TENG) introduced by Wang's group is one such emerging energy harvesting technology, which efficiently converts mechanical energy into electrical energy.[2,3] TENG is based on the coupling of contact electrification and electrostatic induction.[4,5] Contact electrification creates static polarized charges on material surfaces in contact, while electrostatic induction across electrodes transforms mechanical energy into electricity due to Maxwell's displacement current generated by mechanical separation.[6] Its versatility, adaptability, and relatively simple mechanism enable TENG to harvest energy from a variety of sources, such as vibrational,[7] wind,[8] ocean waves,[9] biomechanical,[10] and environmental energy.[11] With a high energy density, easy manufacturing, lightweight, and low cost, TENG is a highly efficient energy harvester for micro-scale applications such as remote sensors for environmental monitoring and self-powered systems for vibration sensing or wireless communication.[12] TENG has attracted a lot of research interest and has been developed rapidly, enabling significant progress in the micro-energy field in the past few years.[13,14]

Most TENGs reported in the literature are based on a solid-solid interface, in which two solid triboelectric materials contact or slide against each other to generate electricity. Over the years, researchers have achieved high and stable output performance from solid-solid TENG by enhancing the nanostructure of solid materials,[15,16] using an external charge pump,[17,18] adopting a multilayer structure,[19,20] and using spring-assisted structures.[21,22] However, the inherent long-term friction between the two solid materials leads to material wear, which reduces its lifetime, making it challenging to sustain long-term operations. Additionally, solid-solid TENG is sensitive to environmental factors, such as air humidity, which causes unstable output when not encapsulated.[23] A solution to these challenges has been found in the liquid-solid interface TENG, where liquid acts as one of the frictional layers contacting the solid layer. The low shape-restriction of liquids and flexibility make liquid-solid

M. Salman, V. Sorokin, Z. Li, K. Aw
Department of Mechanical and Mechatronics Engineering
The University of Auckland
20 Symonds Street, Auckland 1010, New Zealand
E-mail: mmoh803@aucklanduni.ac.nz
Y. Zhu
School of Engineering
University of Southern Queensland
Springfield Central 4300, Australia
W. C. Gan
New Energy Science and Engineering, School of Energy and Chemical Engineering
Xiamen University Malaysia
Sepang 43900, Malaysia

The ORCID identification number(s) for the author(s) of this article can be found under https://doi.org/10.1002/mame.202400159

DOI: 10.1002/mame.202400159

TENGs (LS-TENG) highly effective at capturing environmental energy, including ocean waves. As a result of lower friction between liquid and solid material, LS-TENG overcomes the main disadvantage of solid-solid TENG as they don't wear out solid surfaces, thereby increasing the TENG's lifetime.[24]

Moreover, LS-TENG maximizes the contact area between two triboelectric materials and is moisture-resistant.[25] LS-TENG is characterized by electric double layers (EDL), formed when liquid and solid come into contact.[26,27] According to Wang's model for EDL, the EDL is formed in two distinct steps: in the first step, electrons are exchanged between liquid and solid surfaces, making the atoms on the solid surfaces ions, and in the second step, these ions interact with ions present in the liquid resulting in a gradient distribution of anions and cations near the interface.[26] Ion absorption and electron exchange co-occur during liquid-solid interactions.[27,28]

Several LS-TENGs have been developed in recent years, and this is a growing area of study in the field of TENG. Huang, et al.[29] proposed a rectangular LS-TENG with fluorinated ethylene propylene (FEP) for low-frequency energy harvesting. Based on the results, output performance was strongly affected by the triboelectric material and liquid type, with deionized (DI) water having the highest output. The study discussed that the output was lower for tap water, mineral water, rainwater and river water because of the presence of free ions, which causes a shielding effect. Liang, et al.[30] investigated the effect of different sodium chloride (NaCl) concentrations on the output of an LS-TENG based on dynamic EDL for wave energy harvesting. The results showed that LS-TENG output decreased with increased NaCl concentration as the Na^+ and Cl^- ions are tightly bound on film surfaces, resulting in fewer ions escaping from the surface, leading to lower output. Similarly, Wei, et al.[31] examined the effect of potassium chloride (KCl), sodium sulfate ($NaSO_4$), and NaCl solution on the output of droplet-based LS-TENG with FEP. The results showed that the output decreased as KCl, NaCl and $NaSO_4$ concentrations increased, indicating that salt solutions reduce output. DI water resulted in the highest output as the salt concentration was zero. Luo, et al.[32] developed a probe based on LS-TENG to quantify charges of different polarities at liquid-solid interfaces. Results showed that a significant electrical potential difference between the liquid and electrode allowed the device to quantify interaction charges within 50 ms. Similarly, Liu, et al.[33] proposed a liquid-solid triboelectric probe for the real-time monitoring of sucrose concentration in a solution. The results showed that sucrose in water alters the hydrogen bond in water molecules, which has an adverse effect on the electron transfer in liquid-solid contact electrification. Both these studies provide an understanding of the chemical processes at the liquid-solid contact electrification. Although some studies have examined the impact of certain liquid types and properties on the output performance of LS-TENG, the effect of fluorine and copper ions on the output of LS-TENG has not been reported.

In this study, we aimed to evaluate the effect of fluorine and copper ions on the output of a tubular LS-TENG and examine whether there is a relationship between the charges of liquid and solid materials. The impact of fluorine and copper ions on LS-TENG's output performance was determined using three different concentrations of sodium fluoride (NaF) and copper sulfate ($CuSO_4$) in deionized water (DI NaF and DI-$CuSO_4$). We assessed the effects of DI-NaF and DI-$CuSO_4$ liquid solutions on two oppositely tribo-affinity solid triboelectric materials to see if there is any correlation between them. The two solid triboelectric materials selected were polytetrafluoroethylene (PTFE), a tribo-negative material, and Nylon, a tribo-positive material. This work examines the effect of fluorine and copper ions in the liquid on solid triboelectric material. Therefore, this study will add to further understanding of previously published research results on LS-TENG and provide a better understanding of how ions present in liquid affect the output.

2. Fundamentals of LS-TENG

LS-TENG is based on a free-standing triboelectric mode, which couples contact electrification and electrostatic induction. **Figure 1**a,b illustrates the working principle of LS-TENG with a tribo-negative and tribo-positive solid material with water, respectively. As water slides across the tribo-negative surface, charges are generated on the two materials due to contact electrification. The tribo-negative material will become negatively charged, and the water will be positively charged. Similarly, when water rubs across the tribo-positive material, positive charges will be generated on the solid surface, and negative charges will be generated in the water. The two materials with different electrostatic properties will repeatedly contact and separate as water slides across them, resulting in charge imbalances leading to electron flow and current generation.

If negative or positive ions are introduced into the water, the working principle will differ for the tribo-positive and tribo-negative solid materials. Figure 1c,d shows the working principle of LS-TENG where the water contains some negative ions with tribo-negative and tribo-positive solid material, respectively. Collins[34] discussed that forming a contact ion pair in water requires partial dehydration of positive and negative ions in a salt solution. Negative ions like fluorine (F^-) are strongly hydrated, redistributing the charges in water.[34] With the tribo-negative solid material, the amount of positive charges in the liquid will be lower as some were canceled by the negative ions in the water. Consequently, the number of negative charges generated on the tribo-negative solid material will be lower than that of water without negative ions. Hence, the charge transfer between these two materials will be lower, resulting in a lower output. As water with negative ions slides across the tribo-positive solid material, positive charges will be induced on the surface of the solid material. However, as the water already has some negative ions, contact electrification with the tribo-positive solid material will result in a higher net negative charge. Hence, the charges generated for both materials will increase as they attract each other. Therefore, the charge transfer between the materials will be higher, leading to higher output. It is hypothesized that negative charges in the liquid will have a detrimental effect on the output of a tribo-negative solid material while enhancing the output of a tribo-positive solid material.

Similarly, Figure 1e,f shows the working principle of LS-TENG where water contains some positive ions with tribo-negative and tribo-positive solid material, respectively. The trend observed will be the opposite of that discussed above, whereby the number of charges generated on tribo-negative solid material will be higher than that of water without positive ions, while the number of

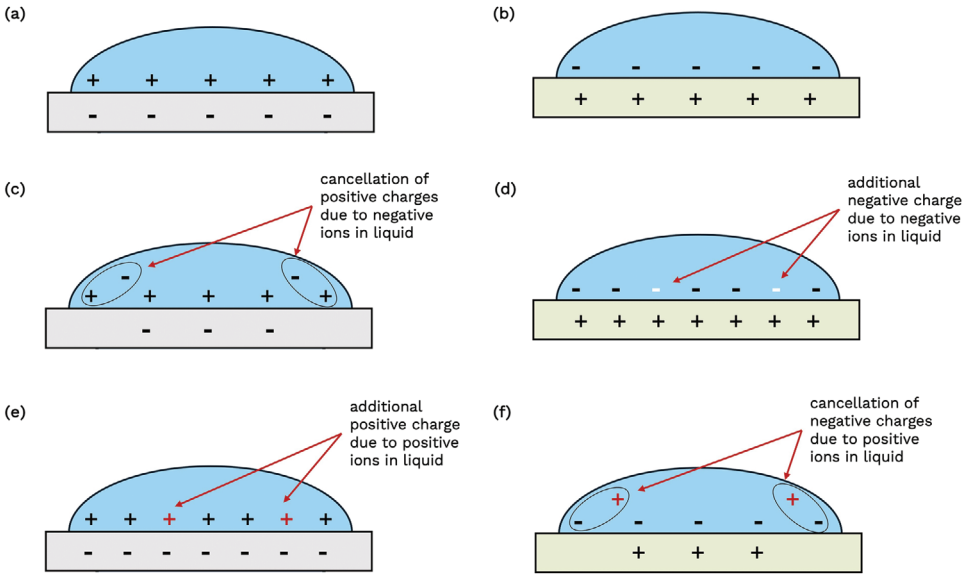

Figure 1. a) Working principle of tribo-negative material with water. b) Working principle of tribo-positive material with water. c) Working principle of tribo-negative material with negatively charged water. d) Working principle of tribo-positive material with negatively charged water. e) Working principle of tribo-negative material with positively charged water. f) Working principle of tribo-positive material with positively charged water.

charges generated on tribo-positive solid material will be lower than that of water without positive ions. Hence, it is hypothesized that positive charges in the liquid will enhance the output of a tribo-negative solid material while having a detrimental effect on the output of a tribo-positive solid material.

3. LS-TENG and Set-Up

Figure 2a,b shows schematic diagrams of PTFE and Nylon LS-TENG, respectively. The LS-TENG comprises a PTFE/Nylon tube with end caps, DI water/DI-NaF/DI-$CuSO_4$ solution, copper (Cu) foil electrodes, and Cu wire. The tube acts as a solid triboelectric material made out of PTFE/Nylon; two symmetrical copper electrodes are placed around the outer surface of the tube. Cu wires connect these electrodes to the electrometer to facilitate output data collection. The top and bottom ends of the tube are covered with end caps to contain the liquid solution. Supporting Information shows a photograph of fabricated PTFE and Nylon LS-TENG in Figures S1 and S2, Supporting Information. PTFE and Nylon tubes were 100 mm long, with an inner diameter of 50 and 1 mm wall thickness. The details on material, fabrication process, and measurement are included in section 6 materials, and methods.

LS-TENG's output was systematically characterized using a seesaw-inspired test platform replicating rocking motion. Figure 2c shows the test platform, where LS-TENG is manually tilted on the seesaw jig. The tilt angle of the seesaw motion was fixed at 26.5 degrees to ensure that both sides rock uniformly, resulting in consistent readings. The same platform was used for PTFE and Nylon LS-TENG to ensure consistency. Figure S3, Supporting Information shows a photograph of the test platform with LS-TENG positioned on the seesaw jig. LS-TENG output was analyzed using DI water, DI-NaF and DI-$CuSO_4$ solutions. Three different concentrations of DI-NaF and DI-$CuSO_4$ solutions were prepared (0.16, 0.36 and 0.56 ppm). Figure 2d shows the conductivity of the solutions. As the concentration of NaF and $CuSO_4$ increases, the conductivity of the DI-NaF and DI-$CuSO_4$ solution increases due to the dissociation of positive and negative ions, which move freely in the solution carrying electrical charges. The presence of these ions in the solution enhances their ability to conduct electricity. It can be seen from Figure 2d that DI water has the lowest conductivity with 6.7 µS, 0.56 ppm DI-NaF solution has the highest conductivity among DI-NaF solutions with 1174.3 µS and 0.56 ppm DI-$CuSO_4$ has the highest conductivity with 449.3 µS among the DI-$CuSO_4$ solutions. The output performance of LS-TENG was analyzed using an electrometer connected to the two copper foils (electrodes) at the test platform, which was manually rocked with the output measured in real-time.

4. Results and Discussions

4.1. Effect of Fluorine and Copper Ions on PTFE LS-TENG

The output performance of PTFE LS-TENG was first evaluated with the three different concentrations of DI-NaF solutions to investigate the effect of fluorine ions. **Figure** 3a shows that as NaF concentration increases, PTFE LS-TENG's open circuit output voltage decreases. The highest output voltage is obtained with DI water as no free ions are in the solution. The decreasing trend of output voltage with DI-NaF solutions may be caused by sodium (Na^+) and F^- ions, which act as free ions in the water. This same trend can be observed in the transferred charge and current output of PTFE LS-TENG with DI-NaF solution illustrated in Figure 3b,c, respectively. Increasing NaF concentration decreased the transferred charge and current, with DI water exhibiting the highest output. Figure 3d depicts PTFE LS-TENG's peak output voltage and charge with DI-NaF solution. The highest peak voltage and charge were observed for DI water at 7.4 V and 2.3 nC, respectively. Meanwhile, 0.56 ppm DI-NaF solution gives the lowest peak voltage and charge, 2.7 V and 0.8 nC,

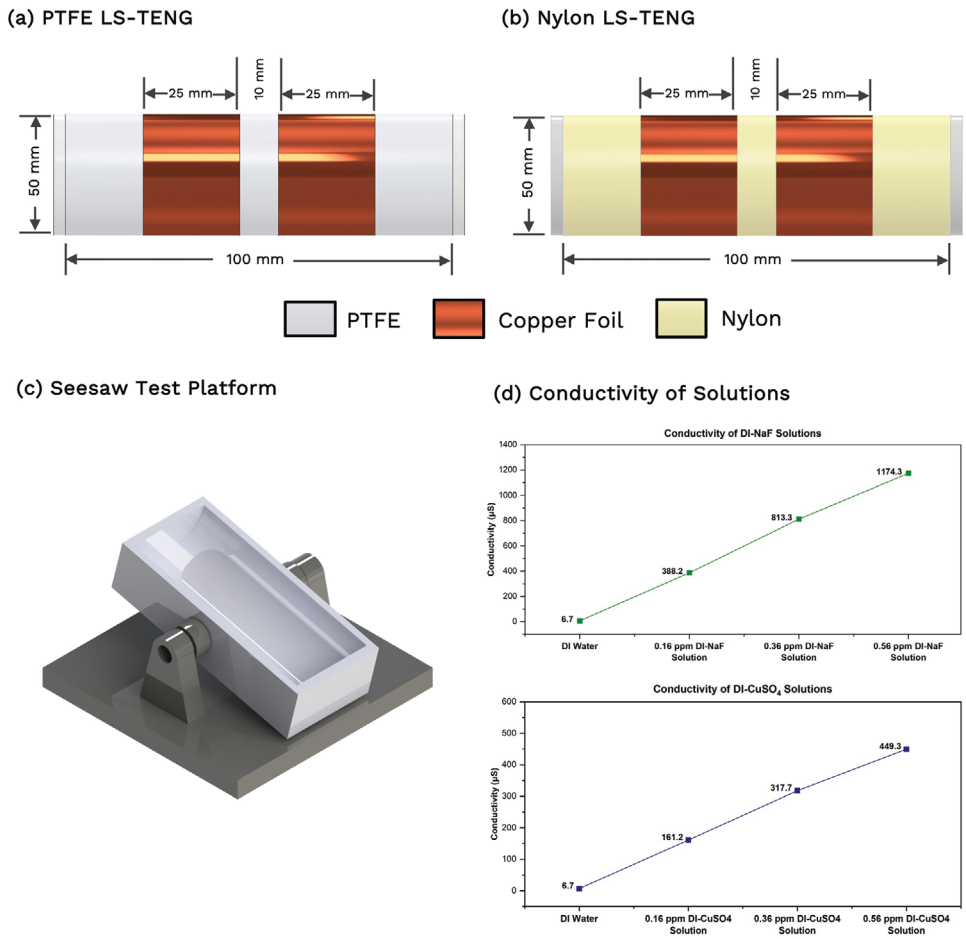

Figure 2. a) Schematic diagram of PTFE LS-TENG. b) Schematic diagram of Nylon LS-TENG. c) Seesaw test platform. d) Conductivity of DI water, DI-NaF and DI-$CuSO_4$ solutions.

respectively. The working mechanism of PTFE LS-TENG with DI water and DI-NaF solution is detailed in Section 2.1 of Supporting Information.

The results show that the output performance of LS-TENG decreases with the introduction of negatively charged F^- ions. This is because the F^- ions in the solution neutralize some positive charges induced in the liquid, diminishing the net charge separation between the two materials. As the concentration of DI-NaF solution increases, the number of F^- ions also increases, leading to an increased neutralization of induced charges. Cao, et al.[35] discussed that the addition of chlorine (Cl^-) salts negatively impacts the output voltage of TENG due to the electronegativity and electrostatic force of ionic compounds, which results in the Cl^- ions getting absorbed on the PTFE surface and neutralizing the induced charge. Similarly, when DI- NaF solution interacts with PTFE, some F^- ions may be absorbed onto the surface of PTFE, affecting the surface charge distribution. Absorption of these ions on PTFE can cause redistribution of surface charges, resulting in lesser charge transfer between the two materials. As NaF concentration increases, more F^- ions are available, which might lead to higher absorption of ions on the PTFE surface, hindering the triboelectric effect. DI-NaF solution may exhibit electrolytic behavior at higher concentrations, allowing F^- ions to move more easily. This might lead to charge neutralization and reduce PTFE's triboelectric effect. The outcome of these is a lower charge transfer between the two materials, resulting in a decrease in the output voltage and charge as the concentration of the DI-NaF solution increases.

The findings are consistent with some of the earlier studies conducted by researchers using NaCl.[30,31,36] These studies showed a decreasing output trend with increased NaCl concentration, primarily attributed to free ions in the solution limiting the charge transfer.[30,31] However, since F^- and Cl^- ions have different chemical properties, they might interact differently with PTFE. For instance, NaF solutions might undergo more ion dissociation than NaCl solutions since fluoride salts are more soluble,[37] resulting in stronger charge neutralization.

The effect of copper ions on the output of PTFE LS-TENG was then examined using the prepared DI-$CuSO_4$ solutions. The PTFE tube was cleaned thoroughly first with isopropanol and then with DI water before conducting experiments with DI-$CuSO_4$ solutions. As shown in **Figure** 4a below, the open circuit output voltage of PTFE LS-TENG increases with an increase in $CuSO_4$ concentration. 0.56 ppm DI-$CuSO_4$ solution produced the highest output voltage, while DI water gave the lowest output voltage. Figure 4b,c shows that the transferred charge and

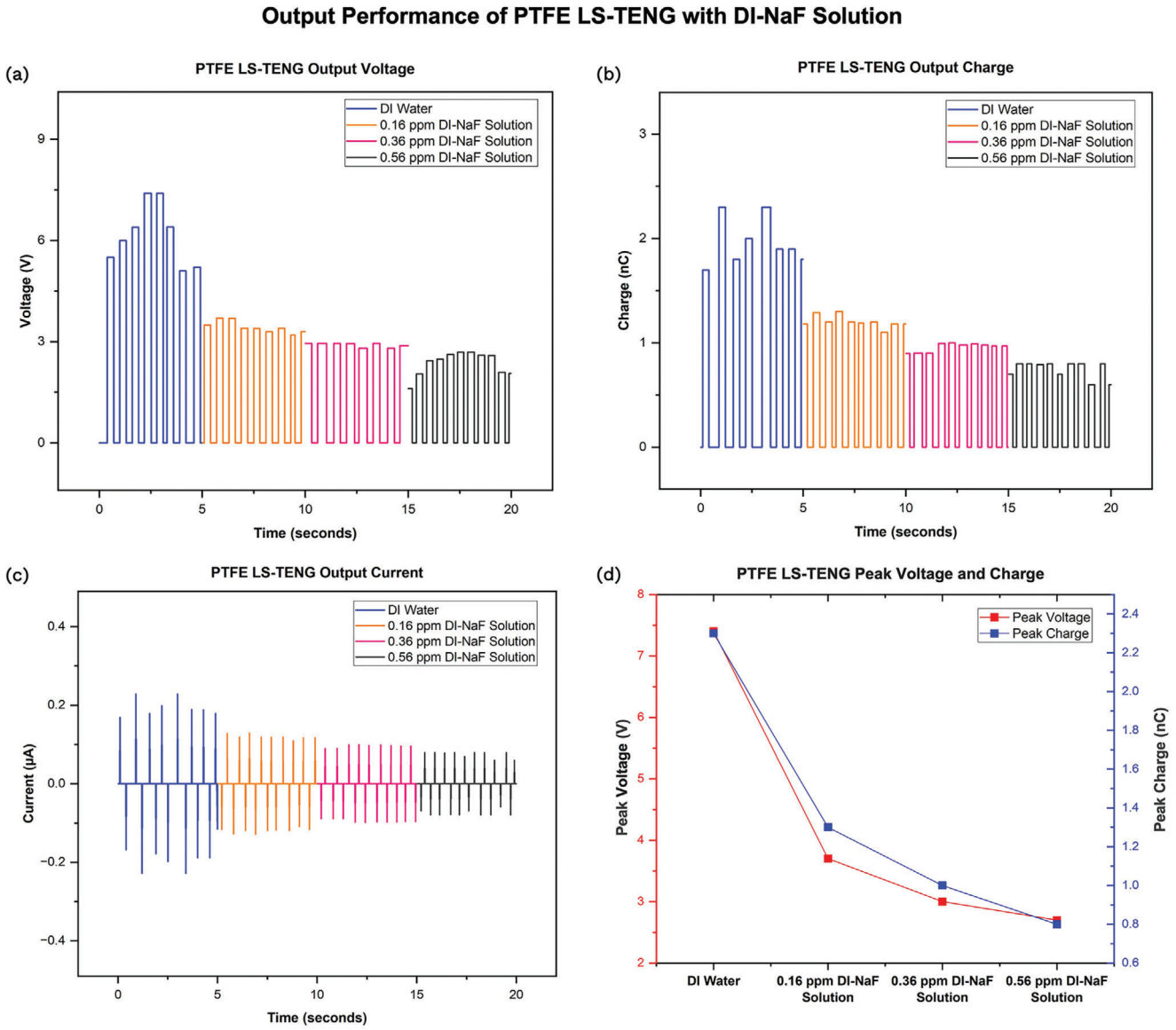

Figure 3. a) Output voltage of PTFE LS-TENG with DI-NaF solution. b) Transferred charge output of PTFE LS-TENG with DI-NaF solution. c) Output current of PTFE LS-TENG with DI-NaF solution. d) Peak output voltage and charge of PTFE LS-TENG with DI-NaF solution.

current output of PTFE LS-TENG with DI-$CuSO_4$ also increases with the $CuSO_4$ concentration. The peak voltage and charge of PTFE LS-TENG with DI-$CuSO_4$ solution are depicted in Figure 4d. 0.56 ppm DI-$CuSO_4$ solution resulted in the highest peak output voltage and charge of 14.7 V and 4.6 nC, while the DI water gave the lowest peak output voltage and charge of 7.4 V and 3.1 nC, respectively.

The results show that PTFE LS-TENG output increases with $CuSO_4$ concentration; this can be attributed to the interaction between the copper (Cu^{2+}) ions in $CuSO_4$ and the tribo-negative PTFE surface. The addition of Cu^{2+} ions in the liquid results in a higher amount of positive charges being generated in the liquid, and as PTFE has the tendency to gain electrons, the interaction between these ions and the PTFE surface results in an enhanced charge transfer, leading to higher output. As the concentration of $CuSO_4$ increases, the number of Cu^{2+} ions in the liquid increases, leading to a more efficient electron transfer and increased output performance. At higher concentrations, the ionic strength of the DI-$CuSO_4$ solution increases, potentially resulting in a stronger electrostatic attraction between the Cu^{2+} ions and the PTFE surface. This leads to a higher surface charge density on PTFE, contributing to a higher potential difference and, thus, higher output. Additionally, PTFE is a chemically inert and hydrophobic material that is strongly resistant to most chemicals.[38] Due to PTFE's nonpolar and inert nature, the Cu^{2+} and sulfate (SO_4^{2-}) ions are unlikely to be absorbed on the PTFE surface. Hence, they do not hinder the charge transfer between the two materials.

According to the results, fluorine F^- ions have a detrimental effect on the output of PTFE LS-TENG, while copper (Cu^{2+}) ions

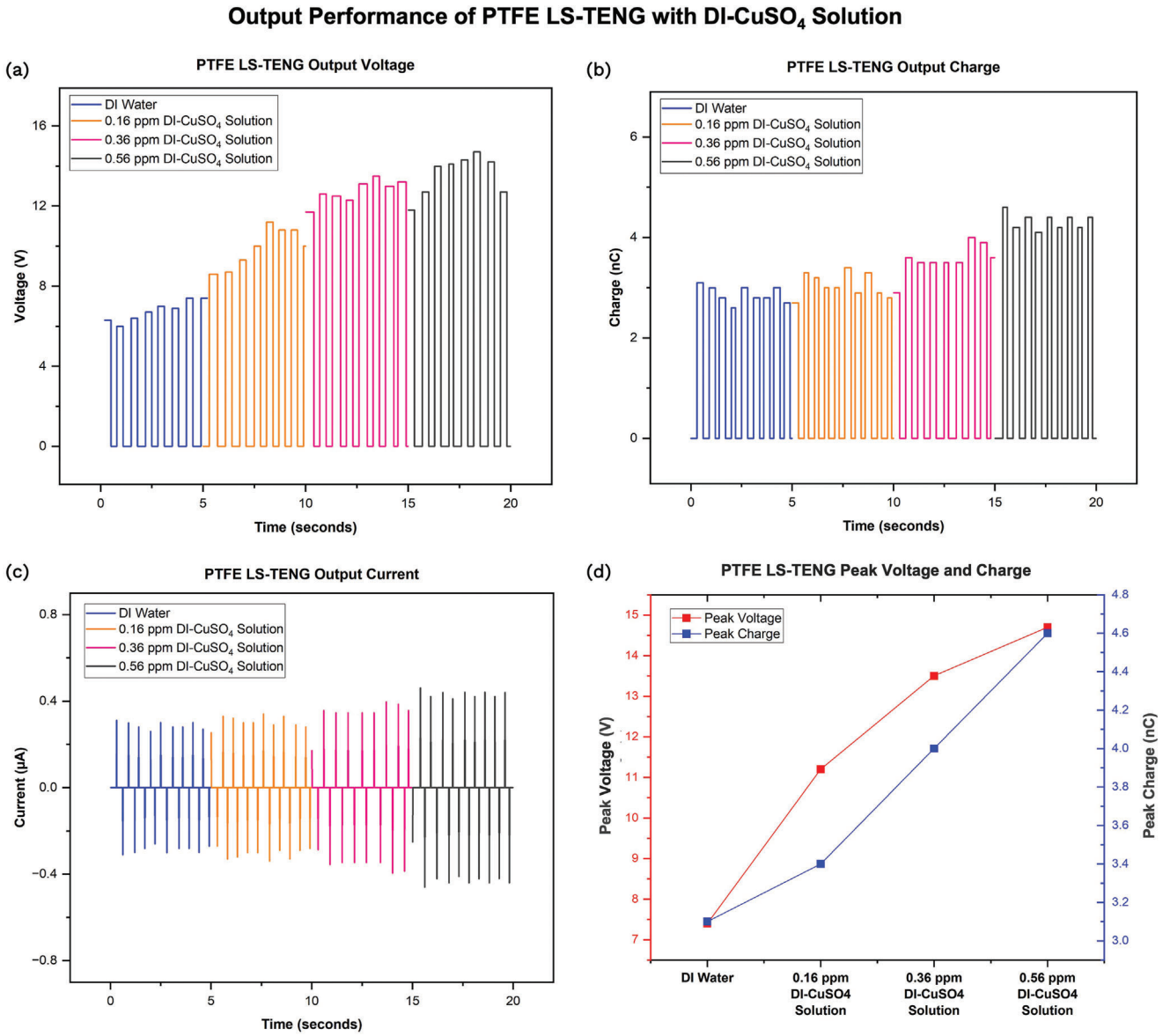

Figure 4. a) Output voltage of PTFE LS-TENG with DI-$CuSO_4$ solution. b) Transferred charge output of PTFE LS-TENG with DI-$CuSO_4$ solution. c) Output current of PTFE LS-TENG with DI-$CuSO_4$ solution. d) Peak output voltage and charge of PTFE LS-TENG with DI-$CuSO_4$ solution.

have a positive effect. The negative impact of F^- ions can be attributed to the neutralization of some positive charges in the liquid and their interaction with the PTFE surface, which leads to surface charge redistribution. On the contrary, the Cu^{2+} ions enhance the output due to their favorable interaction with the PTFE surface, leading to more efficient charge transfer and increased surface charge density.

4.2. Effect of Fluorine and Copper Ions on Nylon LS-TENG

Similar to PTFE LS-TENG, the output performance of Nylon LS-TENG was initially examined with the DI-NaF solutions. The open circuit output voltage of Nylon LS-TENG increases with an increase in NaF concentration, as seen in **Figure** 5a. DI water gives the lowest output voltage, while 0.56 ppm DI-NaF solution provides the highest output voltage. Similarly, Figure 5b,c shows that the transferred charge and current output of Nylon LS-TENG increases with an increase in NaF concentration. The highest transferred charge output is obtained with 0.56 ppm DI-NaF solution. There is a noticeable difference between the trend in Nylon LS-TENG output and that seen in PTFE LS-TENG output, and this is due to the solid material having different electron affinity. Nylon is a tribo-positive material, so the negative F^- ions in the DI-NaF solution favor the output performance. The opposite polarities of these two materials result in higher charge transfer, enhancing the output. Figure 5d illustrates the peak voltage and charge of Nylon LS-TENG with DI-NaF solution. Nylon LS-TENG's peak voltage and charge trends differed significantly from PTFE LS-TENG. 0.56 ppm DI-NaF solution had the

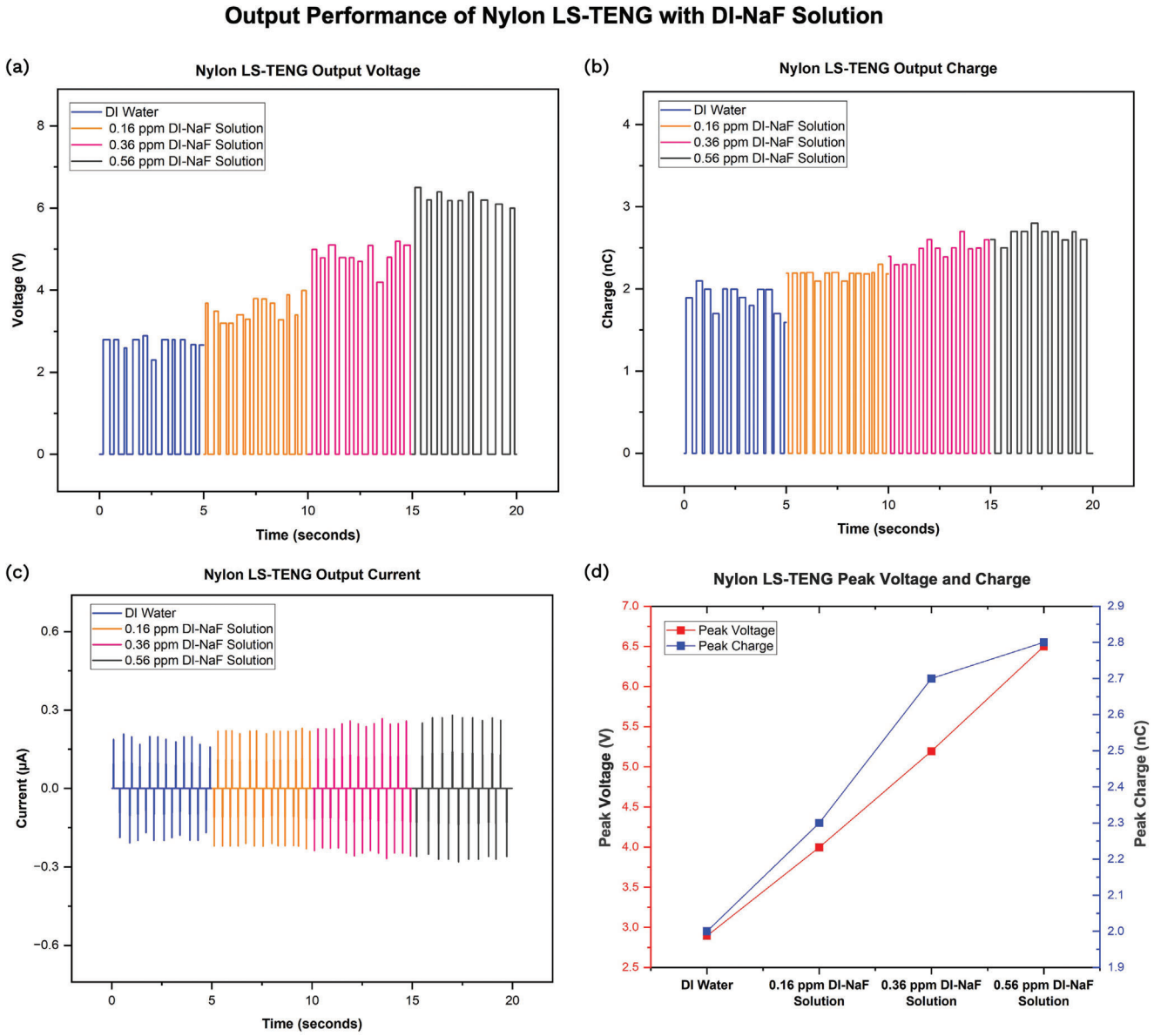

Figure 5. a) Output voltage of Nylon LS-TENG with DI-NaF solution. b) Transferred charge output of Nylon LS-TENG DI-NaF solution. c) Output current of Nylon LS-TENG with DI-NaF solution. d) Peak output voltage and charge of Nylon LS-TENG DI-NaF solution.

highest peak output voltage and charge of 6.5 V and 2.8 nC, while DI water had the lowest peak output voltage and charge of 2.9 V and 2 nC, respectively. Section 2.2 of Supporting Information discusses the working mechanism of Nylon LS-TENG with DI water and DI-NaF solution.

The results indicate opposite trends of PTFE LS-TENG and Nylon LS-TENG with DI-NaF water, with fluorine ions enhancing the output of Nylon LS-TENG while having a negative impact on the output of PTFE LS-TENG. Nylon surfaces could have chemical functionalities that interact with F^- ions more favorably than PTFE, contributing to a stronger triboelectrification effect. For instance, Nylon contains polar groups like amide on its surface.[39] Solomun, et al.,[40] in their study, highlighted that a strong chemical reaction occurs when fluorine and amide groups come into contact, forming polar functionalities. Thus, it is hypothesized that the interaction of F^- ions from DI-NaF solution with Nylon may lead to surface polarization. As a result of polarization, the triboelectric effect can be enhanced, leading to higher output. Additionally, due to more free ions at higher concentrations, the DI-NaF solution exhibits electrolytic behavior,[41] enhancing charge transfer and increasing output voltages. Increased NaF concentration increases output of Nylon LS-TENG due to stronger triboelectric effects, enhanced charge transfer, and polarization on the Nylon surface. To our knowledge, this is the first study exploring Nylon as the solid material for LS-TENG. As these combinations have not been investigated before, we observe that the output performance of Nylon LS-TENG significantly improves with an increase in NaF concentration, indicating that F^- ions are favorable.

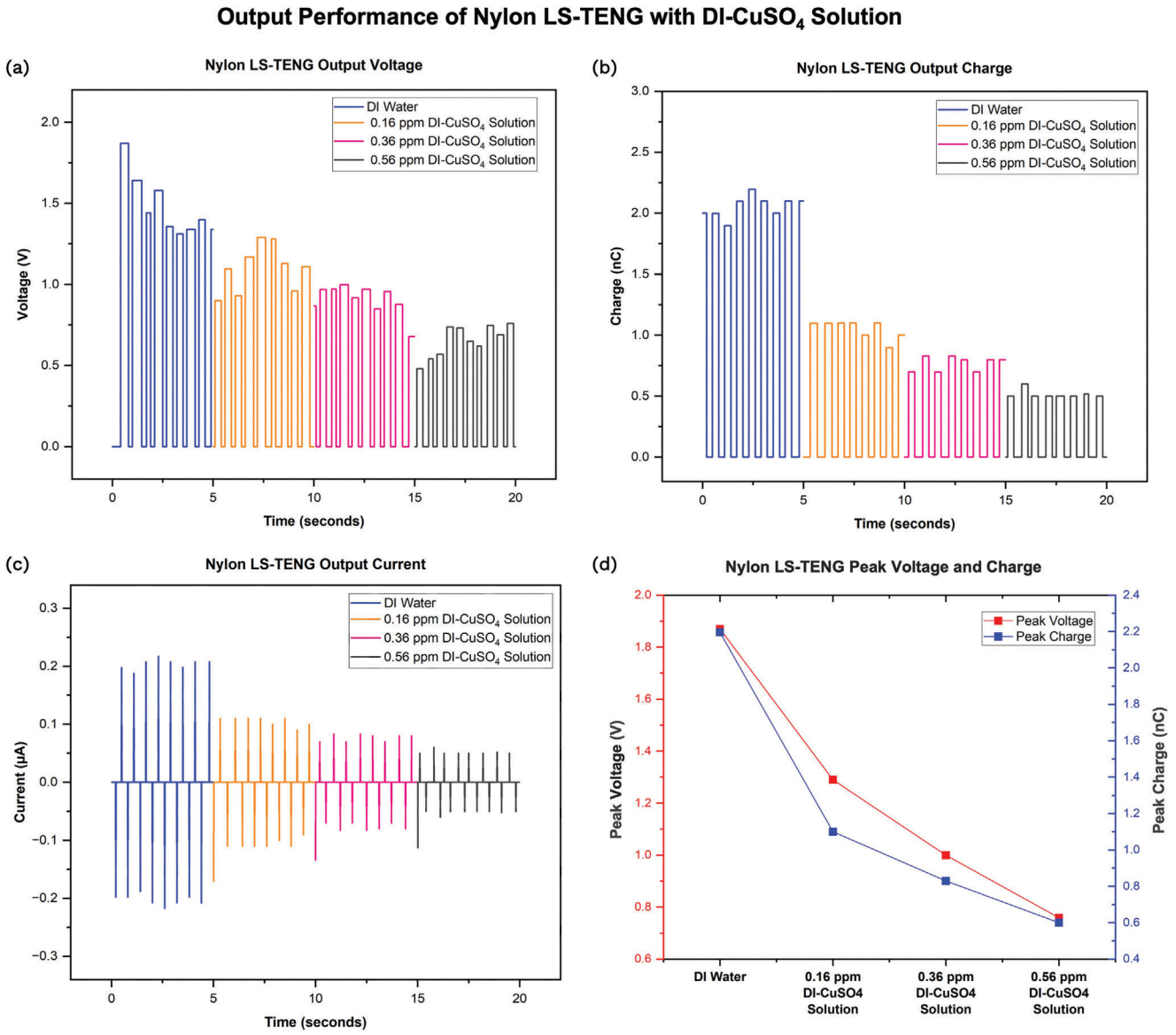

Figure 6. a) Output voltage of Nylon LS-TENG with DI-$CuSO_4$ solution. b) Transferred charge output of Nylon LS-TENG with DI-$CuSO_4$ solution. c) Output current of Nylon LS-TENG with DI-$CuSO_4$ solution. d) Peak output voltage and charge of Nylon LS-TENG with DI-$CuSO_4$ solution.

DI-$CuSO_4$ solutions were then used to evaluate the effect of copper ions on the output performance of Nylon LS-TENG. The Nylon tube was cleaned with isopropanol, and DI water before the experiments with DI-$CuSO_4$ solutions were carried out. **Figure** 6a shows that as $CuSO_4$ concentration increases, Nylon LS-TENG's open circuit output voltage decreases. The highest output voltage is obtained with DI water, while 0.56 ppm DI-$CuSO_4$ solution resulted in the lowest output voltage. A similar trend is observed in the transferred charge and current output of Nylon LS-TENG with DI-$CuSO_4$ solution shown in Figure 6b,c, respectively. An increase in the concentration of $CuSO_4$ resulted in a decrease in transferred charge and current, with DI water giving the highest output. Figure 3d illustrates Nylon LS-TENG's peak output voltage and charge with DI-$CuSO_4$ solution. The highest peak voltage and charge were observed for DI water at 1.9 V and 2.2 nC, respectively. While 0.56 ppm DI-$CuSO_4$ solution resulted in the lowest peak voltage and charge, 0.8 V and 0.6 nC, respectively.

The trend observed from the results is that of decreasing output performance of the Nylon LS-TENG with increasing $CuSO_4$. The number of Cu^{2+} ions increases with the concentration of $CuSO_4$ solution, which neutralizes the negative charges induced in the liquid, resulting in lower charge transfer and output. Additionally, some Cu^{2+} ions may absorb onto the surface of Nylon, which might redistribute the surface charges on the nylon, leading to reduced output. Nylon comprises polar function groups like amide on its surface, allowing ions from the solution to interact with the surface. The positively charged Cu^{2+} can potentially interact with the polar function groups on the surface of nylon, and metal ions have a strong affinity for absorption due

to the formation of coordination bonds,[42] resulting in the Cu^{2+} being absorbed onto the surface. On the contrary, the negative SO_4^{2-} ions in the solution are neutral and less likely to absorb on the surface.[43] As the $CuSO_4$ concentration increases, more Cu^{2+} ions are present in the solution, which may lead to higher absorption of ions on the Nylon surface, reducing the triboelectric effect.

In contrast with the PTFE LS-TENG, the fluorine F^- ions have a positive effect on the output of Nylon LS-TENG, while copper (Cu^{2+}) ions have a negative effect. The electrolytic behavior of DI-NaF solutions at higher concentrations and potential surface polarization due to the interaction between F^- ions with the Nylon surface enhance the triboelectric effect, increasing the output performance. The presence of Cu^{2+} ions in liquid neutralizes some of the charges in the liquid, and the absorption of these ions on the Nylon surface leads to a reduced charge transfer between the two materials, resulting in a lower output.

5. Conclusion

We investigated the effect of fluorine and copper ions on LS-TENG output with PTFE and Nylon as solid triboelectric materials. The findings provide insight into the different effects of fluorine and copper ions on PTFE and Nylon LS-TENG output. The fluorine ions negatively affected PTFE LS-TENG's output, evidenced by the decreased output voltage, charge, and current with increasing NaF concentrations. Meanwhile, fluorine ions positively affected the output of Nylon LS-TENG, leading to an increase in output voltage, charge, and current as NaF concentration increases. Conversely, the copper ions had a positive effect on the output of PTFE LS-TENG and a negative effect on Nylon LS-TENG's output. These results indicate that PTFE and Nylon respond differently to fluorine and copper ions in DI-NaF and DI-$CuSO_4$ solutions due to their material-specific properties. The results show that opposite charges in solid and liquid triboelectric materials enhance output performance by increasing charge transfer, which aligns with the theoretical explanation. In this study, 0.56 ppm NaF in DI water reduces the generated charge to 65% compared to that with only DI water in PTFE LS-TENG and increases the generated charge by 40% in Nylon LS-TENG compared to that with DI water only. A concentration of 0.56 ppm $CuSO_4$ in DI water increases the generated charge by 48% in PTFE LS-TENG compared to that with DI water only and reduces the generated by 73% compared to that with only DI water in Nylon LS-TENG. As a result, this study contributes to a better understanding of the interactions between material and ions in LS-TENG. It also demonstrates the importance of solid and liquid triboelectric material charges on the output. Moreover, the findings provide information for designing LS-TENG tailored for specific applications where the properties of liquids and ions are critical to energy harvesting efficiency. Future research can focus on improving the performance of LS-TENGs across diverse applications through advanced material modifications and structural design.

6. Experimental Section

Material: The PTFE and Nylon tube was 100 mm long, with an inner diameter of 50 mm, an outer diameter of 52 mm, and a 1 mm wall thickness. The PTFE tube was manufactured with Guarniflon Virgin PTFE G400, and the Nylon tube was manufactured using Sustamid Nylon 6G. The tube ends were equipped with 3D-printed end caps. Copper foil tape with a thickness of 50 µm served as the electrode, with electrodes wrapped around the tube with a width of 25 mm each and a distance between them of 10 mm. The DI-NaF solutions were prepared using DI water and NaF powder from Rowe Scientific. The $CuSO_4$ pentahydrate salt from Environmental Control Products (ECP) Ltd and DI water were used to prepare the DI-$CuSO_4$ solution.

Fabrication of LS-TENG: A detailed description of LS-TENG fabrication is shown in supplementary material Figure S4, Supporting Information. PTFE tubes were cleaned with isopropanol; conductive copper foil tape was applied around the outer surface of the tubes with a gap between the electrodes. Thin copper wires were connected to the copper electrode, and a tiny piece of copper tape was wrapped around the other end to connect it to the electrometer. An end cap was used to secure the tube's bottom end. It was then filled with liquid, and the top end of the tube was closed to form a closed cavity.

Measurements: LS-TENG's electrical output, including open-circuit voltage and transferred charge, was measured with a Keithley 6517B electrometer. The electrometer was integrated with LabVIEW, a software developed by National Instruments for logging data in real-time. A seesaw-inspired test platform was 3D printed, as shown in Figure S3, Supporting Information. LS-TENG was placed on the seesaw, and the mechanical motion was manually induced.

Supporting Information

Supporting Information is available from the Wiley Online Library or from the author.

Acknowledgements

The authors thank Léna Bosseray (Ecole Nationale Supérieure d'Ingénieurs de Caen) for her assistance and support with experiments, Joslin Singh (The University of Auckland) for technical advice with chemical solution preparation and lab space, and Sarath Pathirana (The University of Auckland) for technical advice and material procurement.

Open access publishing facilitated by The University of Auckland, as part of the Wiley - The University of Auckland agreement via the Council of Australian University Librarians.

Conflict of Interest

The authors declare no conflict of interest.

Data Availability Statement

The data that support the findings of this study are available from the corresponding author upon reasonable request.

Keywords

charge transfer, copper ions, fluorine ions, liquid-solid, nylon, polytetrafluorethylene, triboelectric nanogenerator

Received: April 29, 2024
Revised: June 18, 2024
Published online: July 15, 2024

[1] A. Hussain, S. M. Arif, M. Aslam, *Renewable Sustainable Energy Rev.* **2017**, *71*, 12.

[2] G. Zhu, B. Peng, J. Chen, Q. Jing, Z. L. Wang, *Nano Energy* **2015**, *14*, 126.
[3] C. Wu, A. C. Wang, W. Ding, H. Guo, Z. L. Wang, *Adv. Energy Mater.* **2019**, *9*, 1802906.
[4] Z. L. Wang, in *Handbook of Triboelectric Nanogenerators*, Springer, Cham. **2023**.
[5] B. K. Yun, H. S. Kim, Y. J. Ko, G. Murillo, J. H. Jung, *Nano Energy* **2017**, *36*, 233.
[6] Z. L. Wang, in *Handbook of Triboelectric Nanogenerators*, (Eds.: Z. L. Wang, Y. Yang, J. Zhai, J. Wang), Springer International Publishing, Cham **2023**.
[7] J. Yang, J. Chen, Y. Yang, H. Zhang, W. Yang, P. Bai, Y. Su, Z. L. Wang, *Adv. Energy Mater.* **2014**, *4*, 1301322.
[8] B. Chen, Y. Yang, Z. L. Wang, *Adv. Energy Mater.* **2018**, *8*, 1702649.
[9] X. Wang, Q. Gao, M. Zhu, J. Wang, J. Zhu, H. Zhao, Z. L. Wang, T. Cheng, *Appl. Energy* **2022**, *323*, 119648.
[10] Y. Zou, V. Raveendran, J. Chen, *Nano Energy* **2020**, *77*, 105303.
[11] Y. Jie, X. Jia, J. Zou, Y. Chen, N. Wang, Z. L. Wang, X. Cao, *Adv. Energy Mater.* **2018**, *8*, 1703133.
[12] W.-G. Kim, D.-W. Kim, I.-W. Tcho, J.-K. Kim, M.-S. Kim, Y.-K. Choi, *ACS Nano* **2021**, *15*, 258.
[13] S. Zhang, M. Bick, X. Xiao, G. Chen, A. Nashalian, J. Chen, *Matter* **2021**, *4*, 845.
[14] D. Jiang, M. Lian, M. Xu, Q. Sun, B. B. Xu, H. K. Thabet, S. M. El-Bahy, M. M. Ibrahim, M. Huang, Z. Guo, *Adv. Compos. Hybrid Mater.* **2023**, *6*, 57.
[15] Y. Zou, J. Xu, K. Chen, J. Chen, *Adv. Mater. Technol.* **2021**, *6*, 2000916.
[16] H. Chen, Y. Xu, J. Zhang, W. Wu, G. Song, *Nano Energy* **2019**, *58*, 304.
[17] Z. Yang, Y. Yang, H. Wang, F. Liu, Y. Lu, L. Ji, Z. L. Wang, J. Cheng, *Adv. Energy Mater.* **2021**, *11*, 2101147.
[18] Y. Bai, L. Xu, S. Lin, J. Luo, H. Qin, K. Han, Z. L. Wang, *Adv. Energy Mater.* **2020**, *10*, 2000605.
[19] Y. Li, Z. Guo, Z. Zhao, Y. Gao, P. Yang, W. Qiao, L. Zhou, J. Wang, Z. L. Wang, *Appl. Energy* **2023**, *336*, 120792.
[20] Q. Zheng, Y. Jin, Z. Liu, H. Ouyang, H. Li, B. Shi, W. Jiang, H. Zhang, Z. Li, Z. L. Wang, *ACS Appl. Mater. Interfaces* **2016**, *8*, 26697.
[21] C. Wu, R. Liu, J. Wang, Y. Zi, L. Lin, Z. L. Wang, *Nano Energy* **2017**, *32*, 287.
[22] T. Jiang, Y. Yao, L. Xu, L. Zhang, T. Xiao, Z. L. Wang, *Nano Energy* **2017**, *31*, 560.
[23] V. Nguyen, R. Zhu, R. Yang, *Nano Energy* **2015**, *14*, 49.
[24] S. Lin, X. Chen, Z. L. Wang, *Chem. Rev.* **2021**, *122*, 5209.
[25] C. Cai, B. Luo, Y. Liu, Q. Fu, T. Liu, S. Wang, S. Nie, *Mater. Today* **2022**, *52*, 299.
[26] Z. L. Wang, *Adv. Energy Mater.* **2020**, *10*, 2000137.
[27] J. Nie, Z. Ren, L. Xu, S. Lin, F. Zhan, X. Chen, Z. L. Wang, *Adv. Mater.* **2020**, *32*, 1905696.
[28] S. Lin, L. Xu, A. Chi Wang, Z. L. Wang, *Nat. Commun.* **2020**, *11*, 399.
[29] T. Huang, X. Hao, M. Li, B. He, W. Sun, K. Zhang, L. Liao, Y. Pan, J. Huang, A. Qin, *ACS Appl. Mater. Interfaces* **2022**, *14*, 54716.
[30] X. Liang, S. Liu, S. Lin, H. Yang, T. Jiang, Z. L. Wang, *Adv. Energy Mater.* **2023**, *13*, 2300571.
[31] X. Wei, Z. Zhao, C. Zhang, W. Yuan, Z. Wu, J. Wang, Z. L. Wang, *ACS Nano* **2021**, *15*, 13200.
[32] B. Luo, T. Liu, C. Cai, J. Yuan, Y. Liu, C. Gao, X. Meng, J. Wang, S. Zhang, M. Chi, Y. Qin, J. Zhao, X. Zhuang, S. Wang, S. Nie, *Nano Energy* **2023**, *113*, 108532.
[33] T. Liu, W. Mo, X. Zou, B. Luo, S. Zhang, Y. Liu, C. Cai, M. Chi, J. Wang, S. Wang, D. Lu, S. Nie, *Adv. Funct. Mater.* **2023**, *33*, 2304321.
[34] K. D. Collins, *Q Rev Biophys* **2019**, *52*, e11.
[35] S. Cao, H. Zhang, X. Cui, Z. Yuan, J. Ding, S. Sang, *Adv. Eng. Mater.* **2019**, *21*, 1800823.
[36] Q. Xu, C. Shang, H. Ma, Q. Hong, C. Li, S. Ding, L. Xue, X. Sun, Y. Pan, T. Sugahara, *Nano Energy* **2023**, *109*, 108240.
[37] J. P. Simmer, N. C. Hardy, A. F. Chinoy, J. D. Bartlett, J. C. Hu, *J Int Soc Prev Community Dent* **2020**, *10*, 134.
[38] E. Dhanumalayan, G. M. Joshi, *Adv Compos Hybrid Mater* **2018**, *1*, 247.
[39] Y. Li, W. A. Goddard, *Macromolecules* **2002**, *35*, 8440.
[40] T. Solomun, A. Schimanski, H. Sturm, E. Illenberger, *Chem. Phys. Lett.* **2004**, *387*, 312.
[41] A. Alva, M. Sumner, W. Miller, *Soil Sci.* **1991**, *152*, 239.
[42] M. Tian, L. Fang, X. Yan, W. Xiao, K. H. Row, *J. Anal. Methods Chem.* **2019**, *2019*, 1948965.
[43] F. J. Millero, D. J. Hawke, *Mar. Chem.* **1992**, *40*, 19.

